A cryptotephra from the Upper Pleistocene volcanism of the Bas-Vivarais in the sedimentary infilling of the Chauvet-Pont d'Arc cave (Ardèche, France)

Jean-François Pastre, Évelyne Debard, Catherine Ferrier, Michel Fialin, Bernard Gély, Bertrand Kervazo, Frédéric Maksud, Fatima Mokadem, Sébastien Nomade, Nicolas Rividi, et al.

Original Article - Stratigraphy, Sedimentology

A cryptotephra from the Upper Pleistocene volcanism of the Bas-Vivarais in the sedimentary infilling of the Chauvet-Pont d'Arc cave (Ardèche, France)

Jean-François Pastre [a]*, Évelyne Debard [b], Catherine Ferrier [c], Michel Fialin [d], Bernard Gély [e], Bertrand Kervazo [f], Frédéric Maksud [g], Fatima Mokadem [a], Sébastien Nomade [h], Nicolas Rividi [d] and Ségolène Saulnier-Copard [a]

[a] Laboratoire de Géographie Physique.UMR 8591 CNRS, Universités de Paris I et XII, 1 place Aristide Briand, 92195 Meudon Cedex, France

[b] 25 rue Paul Chevrel, 69370 Saint-Didier-au Mont d'Or , France

[c] Université de Bordeaux – PACEA, UMR 5199 CNRS-UB-MC, Allée Geoffroy-Saint-Hilaire, CS 5003, 33615 Pessac Cedex, France

[d] Camparis, UPMC, 4 place Jussieu, Tour 46-3ème étage

[e]DRAC Auvergne-Rhône-Alpes, Pôle Patrimoine, Service Régional de l'Archéologie, Le Grenier d'Abondance, 6 quai Saint-Vincent, 69001 Lyon, France

[f] 6, rue du Serment, 24000 Périgueux, France

[g] UMR 5608 – Laboratoire TRACES – SMP3C, Ministère de la culture et de la communication, Direction Régionale des Affaires Culturelles d'Occitanie, Service Régional de l'Archéologie – Pôle de Toulouse, Hôtel Saint-Jean – 32, rue de la Dalbade, BP 811, 31080 Toulouse Cedex 6, France

[h] Laboratoire des Sciences du Climat et de l'Environnement (IPSL-CEA-CNRS-UVSQ) et Université Paris-Saclay, Orme des Merisiers, Bâtiment 714, 91190 Gif-sur-Yvette, France

E-mails: jean-francois.pastre@lgp.cnrs.fr (J.F. Pastre), evelyne.debard@free.fr (É. Debard), catherine.ferrier@u-bordeaux.fr (C. Ferrier), michel.fialin@upmc.fr (M. Fialin), bernard.gely@culture.gouv.fr (B. Gély), bertrand.kervazo@orange.fr (B. Kervazo), frederic.maksud@culture.gouv.fr (F. Maksud), fatima.mokadem@lgp.cnrs.fr (F. Mokadem), Sebastien.Nomade@lsce.ipsl.fr (S. Nomade), nicolas.rividi@upmc.fr (N. Rividi), segolene.saulniercopard@lgp.cnrs.fr (S. Saulnier-Copard)

* Corresponding author.

Abstract

A cryptotephra belonging to the Upper Pleistocene volcanism of the Bas-Vivarais was identified for the first time in the sedimentary infilling of the entrance area of the Chauvet-Pont d'Arc cave. This slightly reworked tephra fall is characterized by its heavy minerals assemblage, among which magnesian olivine, enstatite, and chromian diopside issued from peridotites and olivine and diopside of basaltic origin. This composition likely refers to a phreatomagmatic eruption of a maar-crater. The ^{14}C datings of the cryptotephra beds are contemporaneous with the Aurignacian settlement and paintings, that is, an age slightly older or close to 36 ka. Among the maar-craters from the Bas-Vivarais, the Ray-Pic maar have the closest $^{40}Ar/^{39}Ar$ age (36.2 ± 11.3 / 32.2 ± 11.1 ka). By contrast, the Vestide-du-Pal, the biggest maar-crater of this country, seems to have a younger age, but the $^{40}Ar/^{39}Ar$ dating was measured on a basalt which could have occurred later and been the source of the tephra-fall, since its tephras contain the same minerals of unknown origin as those found in Chauvet Cave. This discovery strengthens the previous hypothesis according to which the humans living in the Chauvet-Pont d'Arc area during the Upper Paleolithic have witnessed eruptions from the Bas-Vivarais volcanic field and other phenomena.

Keywords. Chauvet-Pont d'Arc cave, Cryptotephra, Phreatomagmatism, Bas-Vivarais volcanism, Upper Pleistocene.

Manuscript received 25th February 2021, revised and accepted 22nd March 2021.

1. Introduction

The Chauvet-Pont d'Arc cave is situated in France in the Ardèche valley near Vallon-Pont-d'Arc (44° 23' 14" N, 4' 25' 07" E, Figure 1A, B, D). Discovered in 1994, it is universally known for the richness and the age of its Paleolithic paintings (Clottes, 2001; Clottes and Geneste, 2007, Delannoy and Geneste, 2020). The ^{14}C datings of charcoal and paintings indicate two periods of occupation attributed to the Aurignacian and to the Gravettian (from 37.5 to 33.5 ka cal BP and from 31 to 28 ka cal BP; Clottes et al., 1995; Cuzange et al., 2007; Quiles et al., 2016; Valladas et al., 2005). These dates coincide with one of the activity phases of the Bas-Vivarais volcanism. Several recent $^{40}Ar/^{39}Ar$ datings have actually dated these eruptions between 29 ± 10 ka and 35 ± 8 ka (95% probability uncertainty Nomade et al., 2016, Sasco, 2015, Sasco et al., 2017). These dates fully cover the ^{14}C AMS datings (Quiles et al.,

2016) and the thermoluminescence (TL) datings (Guibert et al., 2015) which correspond to the human settlements responsible for numerous parietal representations in the cave. Among them, spray-shape signs (Figure 1C) were hypothetically ascribed to depiction of strombolian volcanic eruptions (Nomade et al., 2016).

In the context of the pluridisciplinary study of the cave financed by the French Culture Ministry the analysis of the heavy minerals of the sediments was undertaken. This study led to the discovery of volcanic minerals attributed to a cryptotephra subcontemporaneous with the sedimentary infilling of the entrance area of the cave. These results, presented here, corroborate the contemporaneity of the recent volcanism of the Bas-Vivarais with the history of the cave during a period close to its occupation by Aurignacians.

2. Stratigraphical and sedimentological context

The volcanic minerals were identified in the sediments of a limited archeological pit located at about twenty meters from the old entrances which are now filled by deposits related to several processes (Figure 2). Four phases were distinguished in the clogging of the entrance (Debard et al., 2016):

- The first one constitutes the origin of a gravity scree (= lower scree) mainly due to the gelifraction of the porch and entry area, to the mechanical expansion of the vaults as well as to the reworking of old superficial deposits. The spreading of the deposits on about forty meters up to the entrance of the Chamber of the Bear Hollows ("Salle des Bauges") is attributed to mobilization by creep and solifluction.
- The second one also corresponds to a gravity scree (intermediate scree) less expanded than the lower one. Their very similar components suggest a same origin.
- The third phase corresponds to blocks generated by the collapse of the cliff. This collapse mainly occurred in two main phases determined by ^{36}Cl cosmogenic dating (23 500 ± 1 200 and 21 500 ± 1 000 years – Sadier et al., 2012) and gave rise to the definitive cave closure. This set was later covered by fine brown sediments originating from reworking of superficial deposits.
- After the closing of the porch, the ultimate registered events correspond to the desquamation of the equilibrium vaults resulting in small sedimentary clasts, to water runoff, to recent concretions growth, to the settling down of the scree.

The archeological pit (named GE1) carried out between 2006 and 2010 (Gély and Maksud, 2009; Gély et al., 2012) is located in a small gallery connecting the old porch to the Chamber of the Bear Hollows ("Salle des Bauges") and corresponding to one of the natural paths used

by large vertebrates and prehistoric humans (Figure 2). Of small dimensions (50 x 50 cm), 80 cm deep, the pit intersected the lower scree and, near the surface, a gravel of clasts issued from the desquamation of the vault.

Six beds have been defined (Figure 3a, b):

- Bed 1: near the surface, this layer is mainly composed of small plates of desquamation (c.1a). Underneath is found dry gravel of elements righted in counterslope (c.1b). Among the clasts of the first level was a fistulous concretion which was dated by U/Th to 13,315 ± 79 years (Genty, 2008). This dating as well as the one obtained on the stalagmite Chau-stm 8 which seals the scree near the archaeological pit and whose basis is dated at 11,500 ± 170 years (Genty et al., 2005) allow to date this bed between the Bølling-Allerød warming and the beginning of the Holocene (Lateglacial). Level c.1b supplied a flint attributed to the Upper Palaeolithic, a trace of the last human incursion before the porch was finally clogged up and attributed to the Gravettian (31,000-28,000 cal BP; Quiles et al., 2016).
- Bed 2: this bed is a small gravel secondarily packed in a sandy-silty reddish matrix. Some clasts show a soft surface identified as bears' polish. Bed 2b corresponds to the reworking of the uppermost part of bed 3.
- Bed 3: this bed is about 10 cm thick, it is less gravely, with a sandy and micaceous matrix very rich in charcoals responsible of its dark color. This layer contrasts with the reddish color of the remaining part of the sequence. It corresponds to the reworking of hearths probably at the origin of the significant thermal impacts observed close to the archeological pit on the ceiling and the walls (Ferrier et al., 2014). Rubefied clasts or with blackish marks have been found in this bed. Dating of several charcoals (i.e. ranging from 36,000-37,000 cal BP; Quiles et al., 2016) attributes these hearths to the Aurignacian occupancy.
- Bed 4: this bed is divided in two, the upper part corresponding to a small dense gravel with angular granules due to run-off, while its lower part is coarser. The matrix is sandy-silty reddish brown becoming more yellow towards the bottom.
- Bed 5: this bed is made of an angular gravel packed in a red sandy sediment, more silty towards the base. At its base, a charcoal dated from between 36,361 and 34,797 cal. BP (Quiles et al., 2016) is contemporaneous to the first Aurignacian occupation of the cave.
- Bed 6: also, coarse, contains wall elements (one block and clasts) polished by bears. The matrix is more sandy, brownish.

- In beds 2 to 5, the presence of sorted lamellar microstructures and occasionally layered caps at the surface of the clasts shows the role of cold weather (mainly frost periods) in this part of the scree and its spreading by solifluction towards the Chamber of the Bear Hollows.

The volcanic minerals characterizing the Chauvet cryptotephra were identified in the beds 6 to 1b, indicating a reworking of the initial tephra fall from the outside.

3. Material and methods

The mineralogical study was carried out on the 63µm-2mm sand fraction separated by wet sieving in an aqueous solution of sodium hexametaphosphate (dispersant) and removing of carbonates (post-deposition calcite coatings) by HCl 1N/2 hours treatment. Results are based on the study of ten samples distributed in the various beds of the archeological pit. The percentages between the silty-clayey fraction and the clayey fraction characterize clayey-silty sands and clayey-sandy silts. The examination of the light sandy fraction reveals quartz-rich sands (angular or slightly blunt quartz) poor in feldspars, issued from the regional granitic and metamorphic basement. Heavy minerals were separated with bromoform (samples CHAU 1-4 = beds 1b, 2, 3, 4) or with sodium polytungstate (samples CHAU 8-9 = beds 5a and 6, samples ARD 25-28 = beds 3, 4, 5, 6). Thus, they represent the heavy fraction ($d > 2.8$), including some minerals of the basement and all the volcanic minerals potentially present, except possible plagioclases of basaltic origin, not analyzed. These volcanic minerals either correspond to minerals typical of basaltic magma or to mantellic minerals issued from ultramafic xenoliths (peridotites/lherzolites). The percentages of heavy minerals vary between 0.85 and 3% of the sand fraction. The minerals have been identified with a polarization microscope and a binocular lens. In order to establish their frequency, which is slightly variable due to the grain-size of the samples, several samples were counted on a squared grid. To specify their respective characterizations and origins, the various minerals identified by optical study were then analyzed with an electron microprobe. The handpicked minerals were included in epoxy resin and polished with abrasive papers and diamond powders. They were then analyzed with a WDS Cameca SX 100 microprobe at the Camparis center (Sorbonne University, Paris VI/CNRS) with column conditions 15 keV, 10 nA. These results were then compared to those of the analysis performed on minerals issued from tephras or peridotitic nodules from the Upper Pleistocene volcanism of Bas-Vivarais (Ardèche).

4. Mineralogy and characterization of the cryptotephra

The results of the heavy minerals counting of six samples are reported in Table 1 and Figure 4. They make it possible to appraise the frequencies of the various species and possibly to link them to the modal composition of the original host-rocks. All the samples are largely dominated by olivine (73.8 to 89.7%). This one is mainly composed of xenomorph grains which can result from the mechanical fragmentation of peridotites nodules or from basaltic magma. Some automorphic specimens clearly originate from the last. The orthopyroxenes (xenomorph enstatite 3.9-7.6%) and the green clinopyroxenes (xenomorph chromiferous diopside, 2.5-6.6%) then represent minerals characteristic of peridotites xenoliths (e.g. Berger, 1981). The brown clinopyroxene (diopside) only plays a minor role (0.7-2%). It probably originates from a basaltic magma together with other pyroxenes such as those occurring in the alkali basalts from the Massif Central. The brown amphiboles, also little abundant (0.2-2%) are probably peridotites amphiboles as those described by Berger (1981).

These minerals are attributable to a basaltic volcanism rich in peridotites nodules (lherzolites) as well as lower crustal material which can only correspond to the Upper Pleistocene volcanism of the Bas-Vivarais located about 35 km away (e.g. Berger, 1973, 1981, Sasco et al., 2017). They come from a tephra brought by the wind at the probable origin of most of the other drifts (basement silts and sands) and scattered in the cave environment. The homogeneity of the minerals assemblage and the freshness of the minerals (e.g. automorphic olivine) lead one to think that this slightly reworked tephra is subcontemporaneous with the sediments including the latter. Thus, it can be defined as a cryptotephra. This fall probably results from a phreatomagmatic eruption associated with formation of a maar. The explosive products (base-surges and falls) are actually usually rich in peridotites minerals (see discussion). The origin of the fall from a strombolian eruption is much less probable. In fact, this type of eruption effectively produces basaltic ashes and scoriae which are not present in the Chauvet samples and are also generally poor in minerals.

The other heavy silicates are basement minerals which play only a minor role (Table 1). These include garnets (0.7 to 5.9%), andalusite, sillimanite-fibrolite, tourmaline and rutile. They could be alluvial minerals from the Ardèche river, coming from the Massif Central and reworked from old fluvial terraces by run-off or gravity process. But they were more probably brought by the wind. Some could also come from the cryptotephra, the explosive products of the maars being mainly rich in basement minerals. The opaque minerals, little represented (2.5 to 3.6%), correspond either to Fe-Ti oxides issued from the regional basaltic volcanism (magnetite,

205 titanomagnetite), or to silicates and oxides of unknown origin (work in progress), or to rare
206 chromium spinels (about 23% of Cr_2O_3) probably issued from peridotites.
207
208 **5. Microprobe geochemical study of minerals**
209
210 In order to precisely characterize the mineralogy and chemical composition of the minerals, a
211 mineralogical study using an electron microprobe was undertaken and compared with the
212 available analyses (Berger, 1981) and new analyses of proximal volcanic falls (base-surges) as
213 well as peridotites from the Ardèche volcanism. Various characteristic analyses are reproduced
214 on Table 2.
215 Olivines are mainly characterized by the variation of their MgO contents. The analysis of
216 automorphic grains reveals compositions comprised between 43.67 and 46.30% of MgO (Fo =
217 83.1-86.6%). Such compositions, poor in Mg, are typical of basaltic phenocrystals as confirmed
218 by their automorphic habitus. After all the cross-checking we have done, it seems that the limit
219 of composition between basaltic and peridotite olivines is at about 47% MgO. The lowering of
220 magnesium in these basaltic olivines (e.g. Table 2, OL1-2) results in their iron enrichment (FeOt
221 = 12.65-15.39% for the most ones) as shown by the diagram of the figure 5. Except for visibly
222 broken specimens from basaltic origin with MgO contents < 47%, the other xenomorphic
223 olivines are more magnesian (MgO = 47.40–48.96%) and characterize olivines from peridotites
224 (e.g. Table 2, OL3-4, Figure 3). However, these olivines are slightly less magnesian than the
225 olivine from peridotites of the Vestide du Pal and Chambon maars analysed by Berger (1981)
226 which mostly exceed 49% of MgO (48.71-49.82%); but based on six analyses performed on
227 the phreatomagmatic tuff of Vestide. We have noticed that they were less magnesian and
228 compatible with the compositions of the Chauvet cryptotephra (44.57 – 44.98 – 45.37 – 47.08
229 – 47.44 – 48.02% MgO). For comparison, the olivines from the Ray-Pic maar peridotites have
230 compositions varying between 47.89 and 49.50% MgO. The olivines of micro-peridotite
231 enclaves found within the strombolian tuff of Gravenne de Montpezat,were also analyzed. They
232 are slightly more magnesian and mainly exceed 49% MgO. Although small, these variations
233 seem to indicate significant slight differences of composition for the olivines of peridotites
234 xenoliths from the Ardèche volcanism.
235 The orthopyroxenes necessarily come from peridotites of which they are one of the
236 characteristic minerals with MgO contents near 32-33%. These are enstatites $En_{87.8\text{-}89.8}$, $Wo_{0.93\text{-}}$
237 $_{1.27}$ (Figure 6). Their analytical results (e.g. Table 2, EN1-2) are close to those of Berger (1981)
238 concerning the orthopyroxenes of peridotites from the Vestide du Pal and Chambon maars. Like

239 them, they are slightly chromiferous (Cr_2O_3 = 0.22-0.34%). The other orthopyroxenes we
240 analyzed (Ray-Pic maar, Borée maar, Gravenne de Montpezat scoria cone, Moula rockshelter
241 tephra) showed relatively similar compositions.
242 The green clinopyroxene corresponds to the common clinopyroxene of peridotites (Berger,
243 1981). This is chromiferous diopside (calcic clinopyroxene Wo_{45-48}, Figure 5). The results of
244 the ten analyses performed (e.g. Table 2, CD1-2) show slightly less chromium-rich pyroxenes
245 than those analysed by Berger (1981) for peridotites of the Vestide du Pal and Chambon maars:
246 0.54-0.81% compared to 0.75-1.36%. This difference is not explained. Only one sample differs
247 with 1.34/1.48% Cr_2O_3.
248 The brown clinopyroxenes correspond to diopsides $Wo_{44.97-48.30} – En_{40.01-42.34} – Fs_{10.68-13.87}$ (e.g.
249 Table 2 BD1-2, Figure 6). These are basaltic pyroxenes common in the alkali basalts from the
250 Massif Central and attributed to the basaltic magma pulverized by the phreatomagmatic
251 eruption. They show typical amounts of Al_2O_3 (8.51-9.46%), TiO_2 (2.15-2.53%) and FeOt
252 (6.14-7.86%).
253 Analysis of some opaque minerals revealed the existence of several minerals of unspecified
254 origin. The first one presents a chemical composition with 27-34.5% SiO_2, 5-7% K_2O, 15.4-
255 20.3% FeOt, 13.9-17.7% Al_2O_3, 5.8-8.8% MgO, 3.8-4.5% TiO_2. The second one is mainly
256 composed of FeO (67-75% FeOt), but contains low percentages of SiO_2, Al_2O_3, CaO, MnO and
257 P_2O_5 and cannot be ascribed to a true oxide.
258
259 **6. Discussion, origin and possible age of the cryptotephra**
260
261 As previously seen the mantellic minerals (peridotites minerals = magnesian olivine +
262 orthopyroxene + chromiferous diopside) and the basaltic minerals (olivine + brown diopside)
263 characterizing the cryptotephra of the Chauvet-Pont-d'Arc cave can be ascribed without any
264 doubt to a phreatomagmatic eruption related to a maar of the Upper Pleistocene volcanism of
265 the Bas-Vivarais. They were pulverized and mixed by the phreatomagmatic explosions. The
266 absence of basaltic ash (microscoriae) attributable to a strombolian eruption, the mixing of
267 mantellic and basaltic minerals and the lower explosivity of this type of eruption led us to
268 exclude a strombolian eruption at the origin of the cryptotephra.
269 The volcanism of the Bas-Vivarais is known since the work of Faujas de Saint-Fond (1778). Its
270 volcanic products are mainly alkaline basalts derived from a unique enriched mantle source
271 (Chauvel and Jahn, 1984; Downes, 1987). It benefited in particular from the works of Berger
272 (e.g. Berger, 1973, 1981, 2007) and is distinguished by the frequency of its ultramafic xenoliths

(Berger, 1981; Berger and Forette, 1975). It comprises 17 eruptive centers. Its activity is characterized by phreatomagmatic eruptions (maars) preceded or generally followed by a strombolian activity associated with the emission of basaltic flows filling pre-existing valleys. The karst of the Bas-Vivarais, situated to the southeast, is characterized by the importance of its Upper Pleistocene infillings (Debard, 1988, 1997). The signature of volcanic eruptions from the Bas-Vivarais was evidenced in three of these karstic infillings: the Moula rockshelter in Soyons (Debard and Pastre, 2008; Pastre et al., 1994), the Marzal II aven (or Flahault aven) and the Devès du Reynaud aven in Saint-Remèze (Debard and Pastre, 2008). Among them, the in-situ tephra found in Soyons is the more representative example of a phreatomagmatic fall comparable to that detected in Chauvet. Among the recent maars of the Bas-Vivarais four present an explosive activity and can be at the origin of the cryptotephra we described above: the Ray-Pic, the Vestide du Pal, the Chambon and the Sapède (Berger, 1981). This last explosion crater can a priori be excluded, due to its essentially basaltic type (Berger, 1981) as confirmed by our own observations and analyses. Derived tephras are therefore mainly composed of basalt clasts and their olivines are mainly basaltic in composition with 44.01-46.55% MgO (Fo = 86.3-87%). The Chambon maar emitted a base-surge and lahars visible in the Fau valley above the hamlet. The mineralogical and microchemical study shows that these products both contain peridotite and basaltic minerals similar to Chauvet' ones. The peridotites olivines (48.43-48.97% MgO) are however more abundant than the basaltic ones in the sample we analyzed. This maar cut in the basement could have been large enough to disperse widespreadly its products, but, due to little extended dispersal in the proximal area, it was probably less extended than those of the following maars. Among the following eruptions, the Vestide du Pal maar constitutes one of the largest explosive craters in the Massif Central (diameter = 1700 m, Berger, 1973, 1981). It emitted important surges visible in its eastern and southern parts (Suc du Pal). The mineralogical study of these products rich in basement minerals pulverized by explosions, show that they content both peridotite and basaltic minerals. These ones however comprise peridotite olivines (47.05-50% MgO) and peridotite pyroxenes. The basaltic olivines (44.57-45.37% MgO) are rare. However, this composition makes them compatible with the composition of Chauvet cryptotephra ones. The Ray-Pic maar also emitted large surges visible along the road D 215 to the east of the Ray-Pic cascade. The mineralogical study of these tephras also rich in basement minerals shows that they contain basaltic and peridotite minerals. The olivine shows a composition varying between 44.63 and 49.78% MgO (Fo = 85.2-90.9%) which clearly argues for these two origins and compositions close to those of Chauvet.

The cryptotephra-bearing beds are well dated due to the presence of micro-charcoals ascribed to frequenting of the site by Aurignacians. ^{14}C AMS datings gave ages comprised between 36, 361-34,797 (bed c5) and 36,100-34,880 (bed c2a) years cal. BP (Quiles et al., 2016). Thus, the cryptotephra must have an age greater than or close to 36 ka. The Bas-Vivarais volcanism benefited from ^{14}C datings (Berger, 1973, Berger et al., 1975, Berger, 2007), from thermoluminescence datings (Guérin, 1983, Guérin and Gillot, 2007, Sanzelle et al., 2000), from paleomagnetism measurements (Rochette et al., 1993, Sasco, 2015, Sasco et al., 2017) and from K-Ar and $^{40}Ar/^{39}Ar$ datings (Sasco, 2015, Sasco et al., 2017). Among them, the $^{40}Ar/^{39}Ar$ datings (ibid.) seem to be the most accurate. The $^{40}Ar/^{39}Ar$ age of the Vestide du Pal maar would thus be comprised between 25.8 ± 7.7 and 27.2 ± 8.2 ka (ibid.). It would thus belong to the recent phase of the Ardèche volcanism. This age seems too young to fit with the potential age of the Chauvet cryptotephra. Nevertheless, it was performed on a basalt following the phreatomagmatic eruption and not on the tephras coming from the maar explosions. It is also the same for the age of the Chambon maar dated at 18.8 ± 9.6 ka (ibid.). On the other hand the age of the Ray-Pic maar comprised between 36.2 ± 11.3 and 32.2 ± 11.1 ka (ibid) is well compatible with the ^{14}C datings of the beds containing the minerals of the Chauvet cave. This maar belonging to the middle phase of the Bas-Vivarais volcanism could be at the origin of the cryptotephra we discovered. Nevertheless, its products do not contain the peculiar minerals which are currently studied to define their origin (terrestrial or extraterrestrial).

The correlation with the other tephras identified in the karstic infillings of the region can be examined. The tephra of the Devès du Reynaud aven (Debard and Pastre, 2008) is characterized by the presence of basaltic glass and its richness in biotite to which a peculiar provenance can be attributed. This composition is clearly different from the Chauvet cryptotephra. In the Marzal II (or Flahault) the basaltic and mantellic minerals reworked in set 5 (Debard and Pastre, 2008) can also be attributable to a phreatomagmatic emission of the Upper Pleistocene volcanism of Ardèche. The data obtained by biochronology suggest that this fall could belong to the recent or middle phase of Ardèche volcanism. The minerals of this infilling could originate from the same fall as the minerals of the Chauvet cave's cryptotephra or originate from another eruption like those of Vestide du Pal or Chambon. The tephra identified in the Moula rockshelter corresponds to a beautiful in situ phreatomagmatic fall (Debard and Pastre, 2008, Pastre et al., 1994). Rich in basement minerals, it contains both peridotite and basaltic minerals as illustrated by the composition of its olivines varying between 43.97 and 48.87% MgO. Its initial dating around 40 ka (Pastre et al., 1994) was contested according to a TL dating of 72 ± 12 ka (Sanzelle et al., 2000). It is indeed worth noticing that this older age is hardly reconcilable with the

sedimentological and paleoclimatic data suggesting a periglacial context rather than a temperate one such as the Saint-Germain 2 episode (Debard and Pastre, 2008). In the hypothesis of an age close to 40 ka, its correlation with the phreatomagmatic eruption of the Ray-Pic maar is possible. This hypothesis is in any case compatible with the composition of the products identified in these two entities.

7. Conclusion

The cryptotephra from the Chauvet-Pont d'Arc cave provides a new example of tephra-fall from the Upper Pleistocene volcanism of the Bas-Vivarais, trapped in the karst of this area. Its possible attribution to the phreatomagmatic eruption of the Ray-Pic maar could be supported by the mineralogical and geochemical compositions of its products containing mantellic and basaltic minerals. It is also in agreement with the recent $^{40}Ar/^{39}Ar$ datings of the Ardèche volcanism (Sasco, 2015; Sasco et al., 2017), giving an age subcontemporaneous with the beds containing the charcoals well dated by ^{14}C (Quiles et al., 2016) and contemporaneous with the Aurignacian occupation and art, that is slightly older than or close to 36 ka. In the other hand, the cryptotephra could also originate from the Vestide du Pal maar, as it also contains peculiar minerals whose origin is still unknown and which were also found in sedimentary infilling of the Chauvet cave. The discovery of this slightly reworked tephra in this remarkable Paleolithic cave provides an additional evidence of the contemporaneity of the Ardèche volcanism with the Aurignacian occupation of this region. Our findings are however not the bulletproof that will legitimate the hypothesis according which the spray-shape signs of the cave can be ascribed to the first depiction of a volcanic eruption (Nomade et al., 2016), but they surely reinforced the hypothesis that Aurignacians have been the witnesses of volcanic activity in the Ardèche region and that volcanic derived material did fall in the vicinity of Chauvet-Pont d'Arc cave about 36 ka ago.

Acknowledgments

We thank the French Culture Ministry and the ARPA (Association de Recherche Paléoécologique en Archéologie) for their financial support. We are especially grateful to Jean-Michel Geneste, former director of the scientific team of the Chauvet cave who as agreed to fund some of the analyzes and to Carole Fritz (CNRS), actual research manager of the Chauvet

team. Warm thanks are addressed to Jane Reilly for her help in the first English translation of this paper. We are grateful to Hélène Paquet for her review of this paper.

References

Berger, E. (1973). Le volcanisme récent de l'Ardèche, PhD thesis, Univ. Orsay, 402 p.

Berger, E. (1981). Enclaves ultramafiques, mégacristaux et leurs basaltes-hôtes en contexte océanique (Pacifique sud) et continental (Massif central français). Thèse d'Etat, Univ. Paris-sud, Orsay, 470 p.

Berger, E. (2007). Les jeunes volcans d'Ardèche. Sud-Ouest éditions. 2879018293, 187 p.

Berger, E. and Forette, M.C. (1975). Réactions des basaltes alcalins des Causses, du Vivarais et du Velay (France) avec les xénocristaux et les minéraux des enclaves homéogènes. *Bull. Soc. Fr. Mineral. Cristal.,* 98 : 366-373.

Berger, E., Brousse, R. and Maury, R.C. (1975). Age récent (11 770 ± 270 ans BP) des dernières éruptions du Vivarais. *C. R. Acad. Sci., Paris*, Ser.D 280 : 419-422.

Chauvel, C.and Jahn, B.M. (1984). Nd-St isotope and REE geochemistry of alkali basalts from the Massif Central, France. *Geochim., Cosmochim. Acta*., 48 : 93-110.

Clottes, J. (2001). La Grotte Chauvet. L'art des origines, Paris, Seuil Edition, 224 p.

Clottes, J., Chauvet,J.-M., Brunel-Deschamps, É., Hillaire, Ch., Daugas, J.-P., Arnold, M., Cachier, H., Évin, J., Fortin, Ph., Oberlin, C., Tisnerat, N. and Valladas, H. (1995). Les peintures préhistoriques de la Grotte Chauvet-Pont d'Arc (Ardèche, France) : datations directes et indirectes par la méthode du radiocarbone. *C. R. Acad. Sci., Paris*, Ser. IIa 320 : 1133-1140.

Cuzange, M.T., Delqué-Kolic, E., Goslar R., Meiert Grootes, P., Higham, T., Kaltnecker, E., Nadau, M.-J., Oberlin, C., Paterne, M., Plicht, J. van der, Bronk Ramsey, Ch., Valladas, H., Clottes, J. and Geneste, J.-M. (2007). Radiocarbon intercomparaison program for Chauvet Cave. *Radiocarbon,* 49(2) : 339-347.

Debard, É. (1988). Le Quaternaire du Bas-Vivarais d'après l'étude des remplissages d'avens, de porches de grottes et d'abris sous-roche. Dynamique sédimentaire, paléoclimatologie et chronologie. Thèse d'Etat. *Doc. Labo. géol. Lyon*, 103, 317 p.

Debard, É. (1997). Les remplissages karstiques du Bas-Vivarais : karstogénèse, sédimentogénèse et archéologie. *Quaternaire,* 8 : 305-317.

406 Debard, É., Ferrier, C. and Kervazo, B. (2016). Grotte Chauvet-Pont d'Arc (Ardèche) :
407 évolution morphosédimentaire de l'entrée. Implication sur les occupations et sur la
408 conservation des vestiges. *Quaternaire*, 27 (1) : p. 3-14.
409 Debard, É. and Pastre, J.F. (2008). Nouvelles données sur les téphras pléistocènes piégés dans
410 les remplissages karstiques ardèchois (S-E France). *Quaternaire,* 19 (2) : 107-116.
411 Downes, H. (1987). Relationship between geochemistry and textural type in spinel peridotite
412 xenoliths, Massif Central, France. *Earth Planet. Sci. Lett.,* 82: 121-135.
413 Faujas de Saint-Fond, B. (1778). Recherches sur les volcans éteints du Vivarais et du Velay.
414 Joseph Cuchet Édition, Grenoble.
415 Ferrier, C., Debard, É., Kervazo, B., Brodard, A., Guibert, P., Baffier, D., Feruglio, V., Gély,
416 B., Geneste, J.-M. and Maksud, F. (2014). Les parois chauffées de la grotte Chauvet-Pont d'Arc
417 (Ardèche, France) : caractérisation et chronologie. *Paleo,* 25 : 59-78.
418 Gély, B., Boche, E. and Maksud, F. (2012). Rapport triennal 2010-2012. In : Études
419 pluridisciplinaires à la grotte Chauvet-Pont d'Arc (Ardèche). Rapports d'activités 2010-2012
420 (coordinateur J.-M. Geneste) : 215-242.
421 Gély, B. and Maksud, F. (2009). Sondage GE-1 dans la galerie d'entrée - Travaux 2009 et
422 synthèse des résultats 2006-2009. In : Études pluridisciplinaires à la grotte Chauvet-Pont d'Arc
423 (Ardèche). Rapports d'activités triennaux 2007-2009 et Perspectives 2010-2012 (coordinateur
424 J.-M. Geneste) : 211-233.
425 Genty, D. (2008). Datations et analyses isotopiques des stalagmites de la grotte Chauvet du
426 Secteur Rouge. In : Geneste, J.M. (dir.), La grotte Chauvet à Vallon Pont d'Arc (Ardèche).
427 Rapports d'activités 2008 : 155-160.
428 Genty, D., Blamart, D. and Ghaleb, B. (2005). Apport des stalagmites pour l'étude de la grotte
429 Chauvet: datations absolues U/Th (TIMS) et reconstitution paléoclimatique par les isotopes
430 stables de la calcite. In : Geneste, J.M. (dir.), La grotte Chauvet à Vallon-Pont d'Arc : un bilan
431 des recherches pluridisciplinaires. Actes de la séance de la Société préhistorique française,
432 Lyon, 2003. *Bull. Soc. Prehist.Fr.,* 102 (1) : 45-62.
433 Guérin, G. (1983). La thermoluminescence des plagioclases. Méthode de datation du
434 volcanisme, applications au domaine volcanique français : Chaîne des Puys, Mont-Dore et
435 Cézallier, Bas Vivarais. Thèse d'Etat. Université Pierre et Marie Curie, 258 p.
436 Guérin, G. and Gillot, P.Y. (2007). Nouveaux éléments de chronologie du volcanisme
437 pléistocène du Bas-Vivarais, (Ardèche, France) par thermoluminescence. *C.R. Geoscience,* 339
438 : 40-49.

Guibert, P., Brodard, A., Quiles, A., Geneste, J.-M., Baffier, D., Debard, É. and Ferrier, C. (2015). When were the walls of the Chauvet Cave heated? A chronological approach by thermoluminescence. *Quat. Geochronol.,* 29: 36-47, doi 10.1016/j.quageo.2015.04.007.

Nomade, S., Genty, D., Sasco, R., Scao, V., Feruglio, V., Baffier, D., Guillou, H., Bourdier, C., Valladas, H., Reigner, E., Debard, É., Pastre, J.F. and Geneste, J.M. (2016). A 36,000-Year-Old Volcanic Eruption Depicted in the Chauvet-Pont d'Arc Cave (Ardèche, France) ? *Plos One* 11(1): e0146621. Doi:10.1371/journal.pone.0146621.

Pastre, J.F., Debard, É., Chennaoui, K. (1994). Un téphra-repère du volcanisme phréatomagmatique du Vivarais dans la séquence Pléistocène supérieur de l'abri Moula (Soyons, Ardèche, France). *C.R. Acad. Sci. Paris,* Ser. II 319 : 937-943.

Quiles, A., Valladas, H., Bocherens H., Delqué-Kolic, E., Kaltnecker, E., van der Plicht J., Delannoy, J.J., Feruglio, V., Fritz, C., Monney, J., Philipe M., Tosello, G., Clottes, J. and Geneste, J.M. (2016). A high-precision chronological model for the decorated Upper Paleolithic cave of Chauvet-Pont d'Arc, Ardèche, France. PNAS.og.cgi/doi/10,1073/Pnas.1523158113., 6 p.

Rochette, P., Bertrand, H., Braun, C. and Berger, E. (1993). La province volcanique Pléistocène Supérieur du Bas-Vivarais (Ardèche, France) : propagation de fentes crustales en échelons ?. C.R. Acad. Sci. Paris, Ser. II 316 : 913-920.

Sadier, B., Delannoy, J.J., Benedetti, L., Bourlès, D.L., Jaillet, S., Geneste, J.M., Lebatard, A.E.and Arnold, M. (2012). Further constraints on the Chauvet cave artwork elaboration. *Proc. Nat. Acad. Sci. USA*, 109 (21): 8002-8006.

Sanzelle, S., Pilleyre, T., Montert, M., Fain, J., Miallier, D., Camus, G. Goër H. de and Defleur, A. (2000). Datation par thermoluminescence : étude d'une corrélation possible entre le maar de la Vestide-du-Pal et un niveau de téphra de la Baume-Moula-Guercy (Ardèche, France). *C.R. Acad. Sci. Paris*, Ser. II, 330 : 541-546.

Sasco, R. (2015). Développement d'un outil chronostratigraphique pour les archives climatiques : datations absolues (K/Ar, $^{40}Ar/^{39}Ar$) et paléomagnétisme appliqués aux laves. Thèse de doctorat, Université Paris-sud.

Sasco, R., Guillou, H., Nomade, S., Scao, V., Maury R.C., Kissel, C. and Wandres, C. (2017). ^{40}Ar /^{39}Ar and unspiked ^{40}K-^{40}Ar dating of upper Pleistocene volcanic activity in the Bas-Vivarais (Ardèche, France). *J. Volcanol. Geotherm. Res*., 341: 301-314.

Valladas, H., Tisnerat-Laborde, N., Cachier, H., Kaltnecker, E., Arnold, M., Oberlin, C. and Evin J. (2005). Bilan des datations carbone 14 effectuées sur des charbons de bois de la grotte Chauvet. *Bull. Soc. Préhist. Fr.*,102 (1) : 109-113.

Figures and tables captions

Fig. 1. A) Location of the Chauvet cave in France, B) Location of the Chauvet cave in Ardèche area, C) Example of spray-shape sign, D) Perspective view of the Bas-Vivarais volcanism seen from Chauvet cave.

Fig. 2. Location of the archeological pit GE1 located about twenty meters from the Palaeolithic entrances. Équipe Grotte Chauvet (Ministère de la Culture, CNRS, Universités).

Fig. 3a. Archaeological pit GE1: view of the southern and western sections and dating elements. Picture by C. Ferrier (Equipe Grotte Chauvet – Ministère de la Culture, CNRS, Universités).
Fig. 3b. Log of the archeological pit GE1.

Fig. 4. Heavy minerals composition of the beds containing the cryptotephra.

Fig. 5. MgO/total FeO diagram of the olivines of Chauvet cryptotephra.

Fig. 6. Wo-En-Fs diagram of the pyroxenes of Chauvet cryptotephra.

Tab. 1. Heavy minerals spectras of samples containing Chauvet cryptotephra.

Tab. 2. Selected microprobe analyses of minerals issued from Chauvet cryptotephra (sample CHAU 4, bed 4). OL1-2: basaltic olivine – OL3-4: peridotite olivine – EN1-2: enstatite – CD1-2: chromiferous diopside – BD1-2: brown diopside. Olivines: numbers of ions on the basis of 4 O, pyroxenes: numbers of ions on the basis of 6 O.

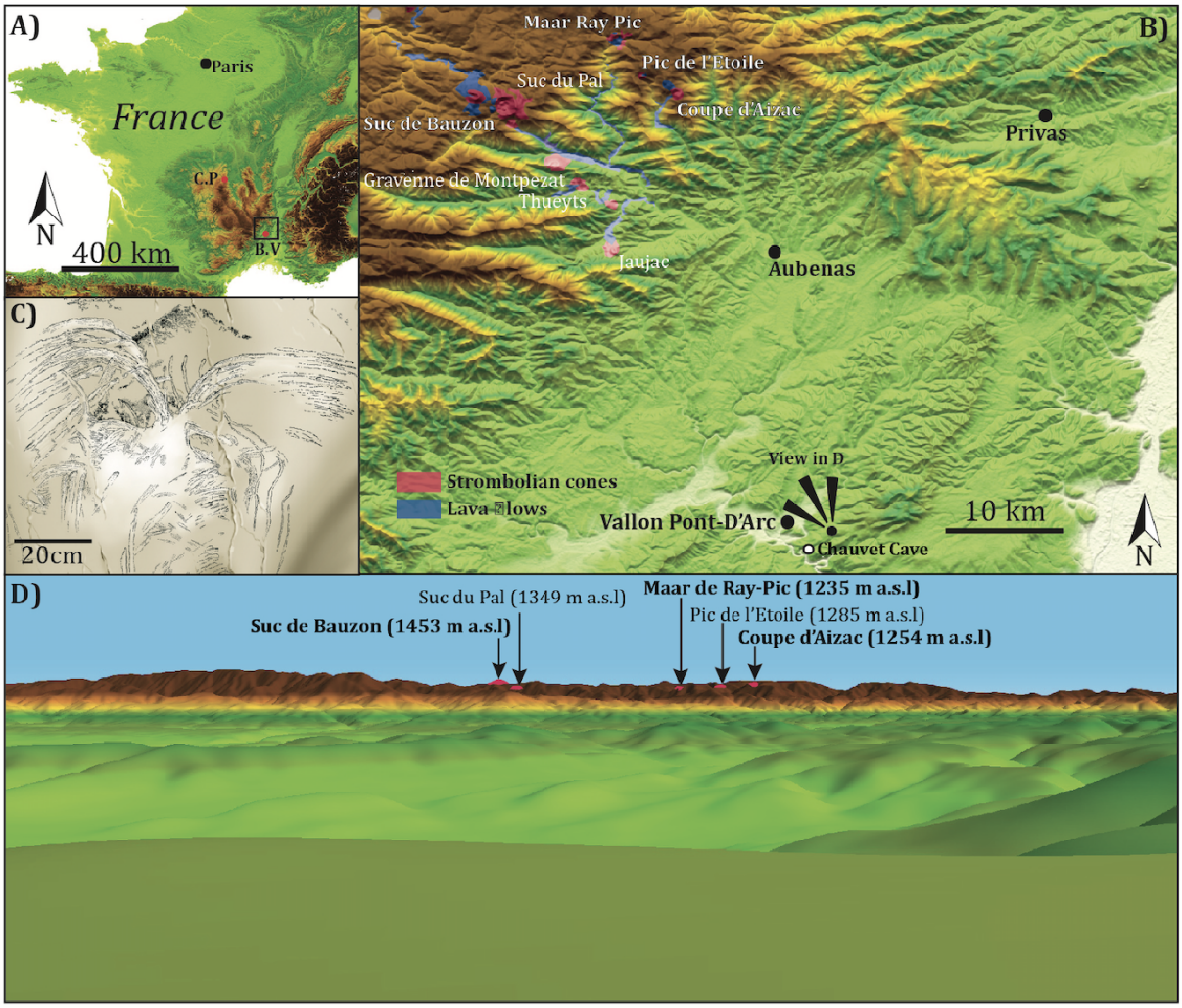
A)
Paris
France
C.P
B.V
N
400 km
B)
Maar Ray Pic
Pic de l'Etoile
Suc du Pal
Coupe d'Aizac
Suc de Bauzon
Privas
Gravenne de Montpezat
Thueyts
Jaujac
Aubenas
C)
20cm
Strombolian cones
Lava flows
View in D
Vallon Pont-D'Arc
Chauvet Cave
10 km
N
D)
Suc du Pal (1349 m a.s.l)
Suc de Bauzon (1453 m a.s.l)
Maar de Ray-Pic (1235 m a.s.l)
Pic de l'Etoile (1285 m a.s.l)
Coupe d'Aizac (1254 m a.s.l)

501

502 Fig. 1


N
13-La Sacristie
12-Le Belvédère
11-Salle du Fond
9-Galerie des Croisillons
10-Galerie du Mégacéros
8-Salle du Crâne
7-Salle Hillaire
6-Galerie du Cierge
4-Galerie des Panneaux rouges
5-Galerie du Cactus
3-Salle des Bauges
2-Salle Brunel
1-Salle Morel
Archaeological pit GE1
Palaeolithic entrance
0 2m
0 10 20
Mètres
Echelle 1:900
Source : Chauvet research team - 2019
Topography made from the 3D scan (0,05 cm)

503

504 Fig. 2

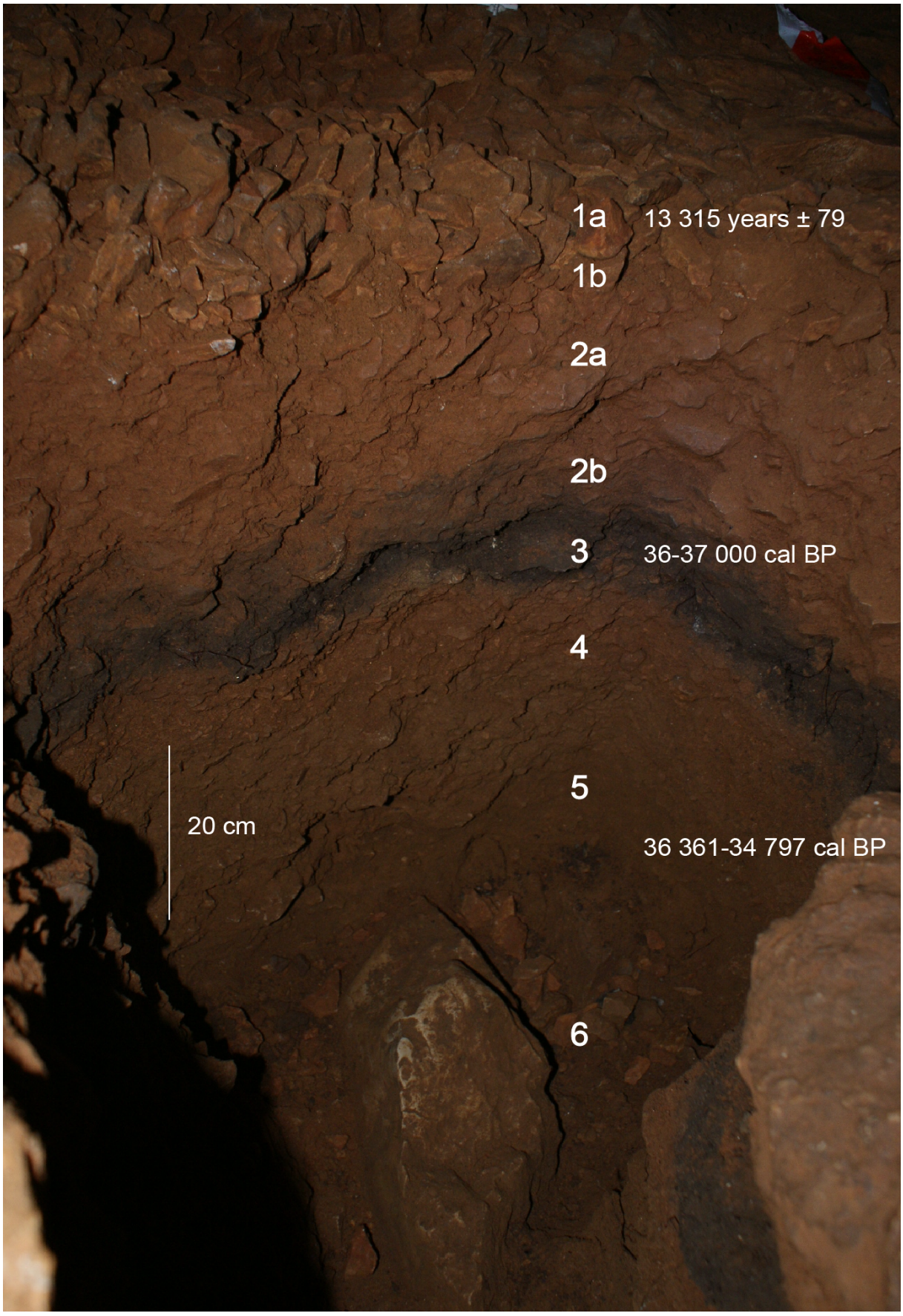

505

506 Fig. 3a

507

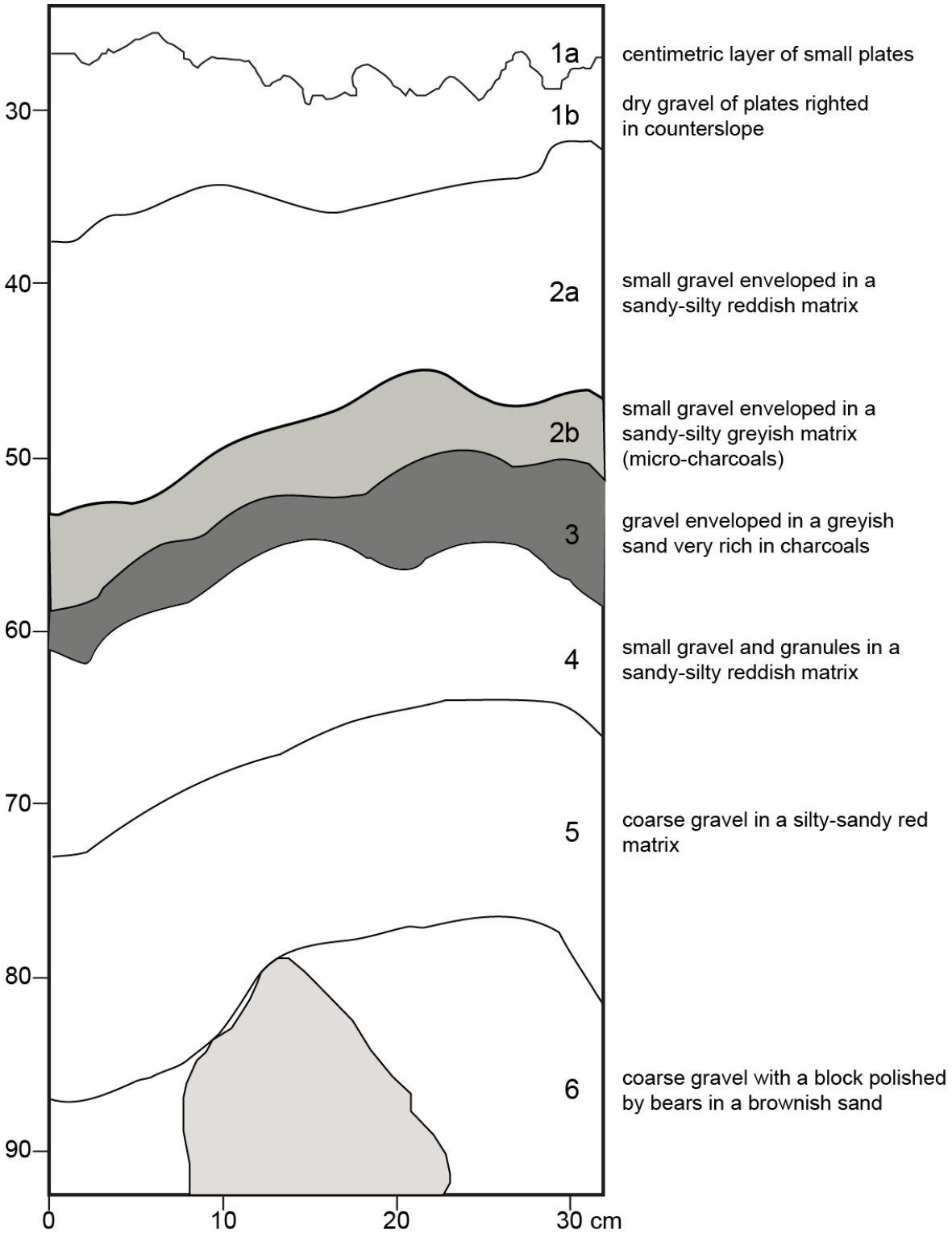

508

509 Fig. 3b

510

511

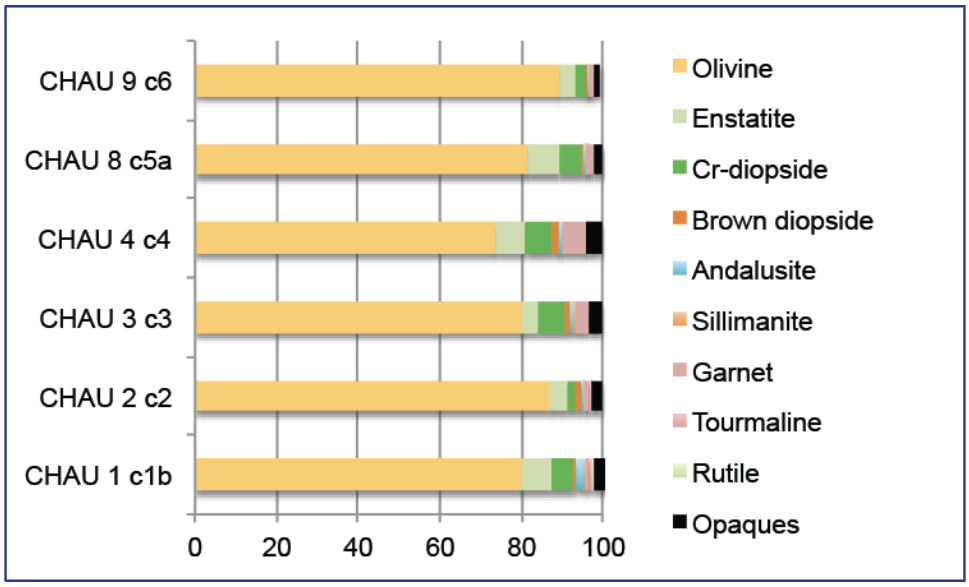

512

513 Fig.4

514

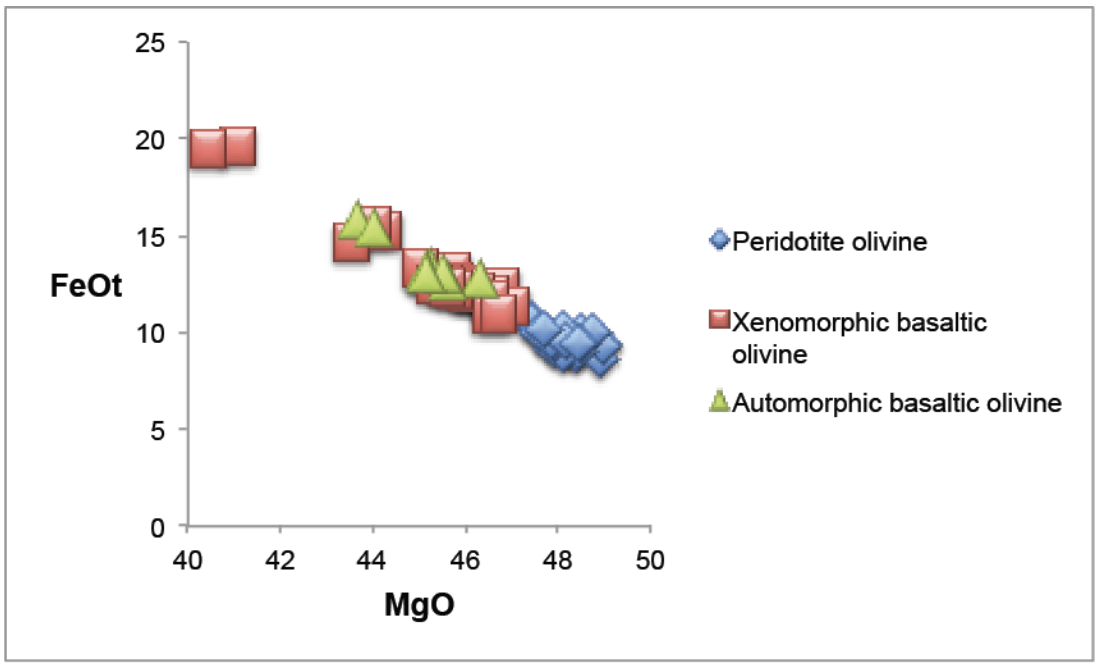

515

516 Fig. 5

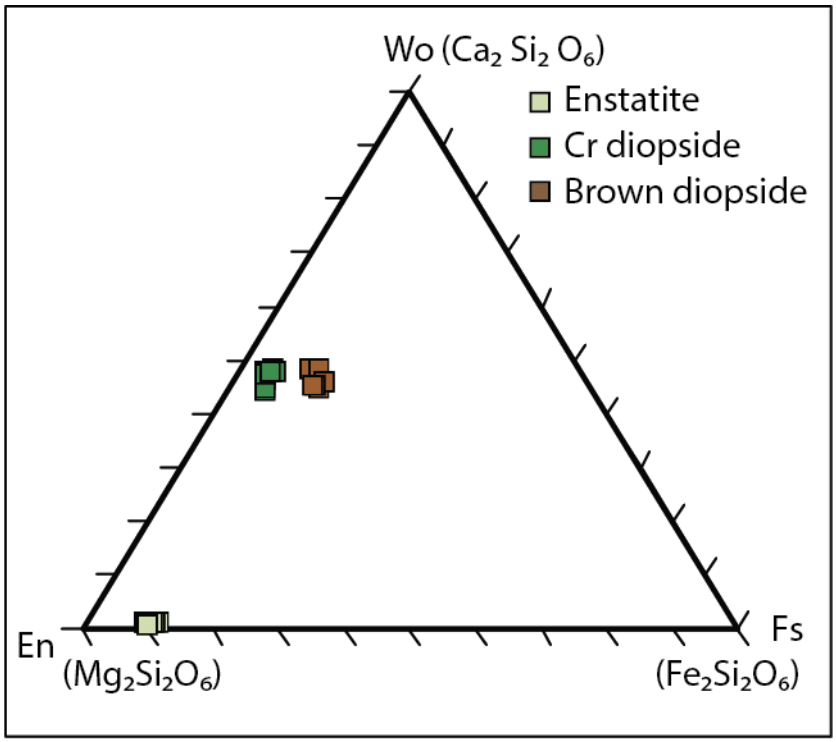

517

518 Fig. 6

519

Sample Bed	CHAU 1 1b	CHAU 2 2	CHAU 3 3	CHAU 4 4	CHAU 8 5a	CHAU 9 6
Brown amphibole	2.01	0.25	0.39	0.28	0.99	0.51
Enstatite	7.38	4.28	3.9	7.26	7.58	3.78
Chromiferous diopside	5.37	2.52	6.64	6.14	5.58	2.41
Brown diopside	0.67	1.26	1.17	1.95	0.39	0.34
Olivine	77.18	86.64	80.07	73.74	80.43	89.5
Andalusite	2.01	0.75	0.78	0.83	0.59	0.34
Sillimanite-fibrolite	0.67		0.39		0.39	0.17
Garnet	0.67	1.26	3.51	5.86	1.79	1.37
Tourmaline	0.67	0.5		0.28		
Rutile	0.67					
Opaques	2.68	2.52	3.12	3.63	2.19	1.37

520 Tab. 1

521

	OL1	OL2	OL3	OL4	EN1	EN2	CD1	CD2	BD1	BD2
SiO_2	39.99	40.15	40.96	40.62	56.04	55.48	52.49	52.88	46.68	45.86
Al_2O_3	0.03	0.01	0.10	0.01	3.30	3.40	4.30	4.88	8.80	8.88
TiO_2	0.00	0.03	0.00	0.04	0.04	0.08	0.33	0.24	2.18	2.53
Cr_2O_3	0.00	0.03	0.02	0.02	0.19	0.29	0.81	0.65	0.05	0.07
FeOt	12.72	13.08	9.95	9.38	7.37	6.21	2.71	2.34	6.14	7.86
MnO	0.18	0.13	0.18	0.14	0.16	0.09	0.02	0.02	0.13	0.20
MgO	46.30	45.74	48.50	48.96	32.69	32.22	16.47	15.77	13.28	12.83
CaO	0.18	0.19	0.03	0.07	0.55	0.63	21.75	21.65	21.62	20.23

Na_2O	0.05	0.00	0.02	0.00	0.08	0.06	1.04	1.37	0.75	0.98
NiO	0.33	0.24	0.29	0.34	0.02	0.07	0.02	0.02	0.01	0.05
Total	99.84	99.65	100.12	99.61	100.48	99.58	99.98	99.85	99.71	99.53
Si	0.997	1.003	1.003	0.998	1.933	1.923	1.905	1.916	1.736	1.721
Al	0.001	0.000	0.003	0.000	0.134	0.139	0.181	0.208	0.386	0.392
Ti	0.000	0.000	0.000	0.000	0.001	0.002	0.009	0.006	0.061	0.071
Cr	0.000	0.000	0.000	0.000	0.005	0.008	0.023	0.018	0.001	0.002
Fe	0.265	0.273	0.203	0.192	0.212	0.180	0.082	0.071	0.191	0.246
Mn	0.003	0.002	0.003	0.002	0.004	0.002	0.000	0.000	0.004	0.006
Mg	1.720	1.703	1.77	1.794	1.680	1.716	0.891	0.852	0.736	0.718
Ca	0.004	0.005	0.000	0.002	0.020	0.023	0.846	0.840	0.862	0.813
Na	0.002	0.000	0.001	0.000	0.005	0.004	0.073	0.096	0.054	0.071
Ni	0.006	0.005	0.005	0.006	0.000	0.002	0.000	0.000	0.000	0.001
Total	3.003	2.995	2.995	2.999	3.999	4.002	4.018	4.011	4.035	4.045
Fo	86.6	86.2	89.7	90.3						
Wo					1.06	1.22	46.49	47.65	48.17	45.74
En					87.81	89.4	48.98	48.31	41.14	40.38
Fs					11.11	9.37	4.52	4.02	10.68	13.87

522 Tab. 2